Stem Cell Rev and Rep (2016) 12:560–572
DOI 10.1007/s12015-016-9671-7

Effects of Human Fibroblast-Derived Extracellular Matrix on Mesenchymal Stem Cells

Yaxian Zhou[1,2] · Michael Zimber[3] · Huihua Yuan[1,4] · Gail K. Naughton[3] · Ryan Fernan[3] · Wan-Ju Li[1,2]

Published online: 24 June 2016

Abstract Stem cell fate is largely determined by the microenvironment called niche. The extracellular matrix (ECM), as a key component in the niche, is responsible for maintaining structural stability and regulating cell proliferation, differentiation, migration and other cellular activities. Each tissue has a unique ECM composition for its needs. Here we investigated the effect of a bioengineered human dermal fibroblast-derived ECM (hECM) on the regulation of human mesenchymal stem cell (hMSC) proliferation and multilineage differentiation. Human MSCs were maintained on hECM for two passages followed by the analysis of mRNA expression levels of potency- and lineage-specific markers to determine the capacity of MSC stemness and differentiation, respectively. Mesenchymal stem cells pre-cultured with or without hECM were then induced and analyzed for osteogenesis, adipogenesis and chondrogenesis. Our results showed that compared to MSCs maintained on control culture plates without hECM coating, cells on hECM-coated plates proliferated more rapidly with a higher percentage of cells in S phase of the cell cycle, resulting in an increase in the $CD90^+/CD105^+/CD73^+/CD45^-$ subpopulation. In addition, hECM downregulated osteogenesis and adipogenesis of hMSCs but significantly upregulated chondrogenesis with increased production of collagen type 2. In sum, our findings suggest that hECM may be used to culture hMSCs for the application of cartilage tissue engineering.

Keywords Extracellular matrix · Mesenchymal stem cell · Dermal fibroblast · Chondrogenesis · Cartilage

Introduction

Aging of the musculoskeletal system such as loss of bone density, changes in cartilage thickness and components, and reduction of muscle mass and strength [1, 2] may lead to the development of degenerative diseases [3, 4]. Mesenchymal stem cells (MSCs) are a promising cell source for tissue engineering and regenerative medicine since they have the capacity of self-renewal and multilineage differentiation into cells of both mesodermal and non-mesodermal origin, such as chondrocytes, osteocytes, adipocytes, and neurons [5, 6]. Mesenchymal stem cells are now extensively used in many ongoing clinical trials, even though the mechanisms underlying how MSCs repair damaged tissue are still poorly understood [7–10]. Pre-clinical research has shown a bright prospect of MSC-based therapies for certain diseases. For example, the efficacy of MSC transplantation for cartilage repair has been demonstrated in goat, rabbit and sheep models with cartilage defects [11–13].

To date, there are more than 576 clinical trails registered to investigate the potential of MSCs for disease treatment. One of the unresolved challenges with the use of MSCs for therapies is how to effectively expand MSCs in culture while maintaining MSC phenotypes, properties, and functions. The

Electronic supplementary material The online version of this article (doi:10.1007/s12015-016-9671-7) contains supplementary material, which is available to authorized users.

✉ Wan-Ju Li
li@ortho.wisc.edu

[1] Department of Orthopedics and Rehabilitation, Laboratory of Musculoskeletal Biology and Regenerative Medicine, University of Wisconsin-Madison, 1111 Highland Avenue, WIMR 5051, Madison, WI 53705-2275, USA

[2] Department of Biomedical Engineering, University of Wisconsin-Madison, Madison, WI, USA

[3] PUR Biologics, Irvine, CA, USA

[4] College of Chemistry, Chemical Engineering & Biotechnology, Donghua University, Shanghai, China

procedure of cell culture is required for MSC expansion but unavoidably introduces factors that may change cells in culture. To tackle this issue, research strategies such as use of low oxygen [14, 15] and addition of growth factors [16, 17] or extracellular matrix (ECM) proteins [18] have been applied to improve culture conditions.

The ECM provides not only a structural support but also physical, mechanical and chemical cues to regulate MSC activities [19–23]. Culture coated with a single ECM protein coating has been studied for the potential of maintaining or improving the properties of MSCs during an in vitro culture process [24, 25]. Although the approach of single protein coating is able to facilitate MSC proliferation and differentiation, it still falls short of replicating biological properties and functions of the ECM in MSC niches. Alternatively, Matrigel, a commercialized basement membrane matrix extracted from Engelbreth-Holm-Swarm (EHS) mouse sarcoma, has been widely used for the culture of human embryonic stem cells (hESCs) [26]. Recent studies showed that Matrigel has the ability to maintain self-renewal and pluripotency of stem cells [27, 28]. However, Matrigel may introduce unexpected xenogeneic contaminants and cause pathogen transmission, which limits its application for clinical therapies. Another type of multi-protein ECM that has been used to maintain MSC properties in vitro is decellularized ECM. The process of preparing decellularized ECM allows cells to be removed from a cellular sheet formed in culture, leaving only ECM components behind. Ng et al. have shown that fetal MSC-derived ECM enhances the proliferation and differentiation potential of adult MSCs with the use of decellularized ECM [29]. He and his coworkers have also found that ECM deposited by bone marrow MSCs (BM-MSCs) promotes cell proliferation but reduces levels of intracellular reactive oxygen species. Moreover, decellularized ECM is able to facilitate hepatic differentiation of BM-MSCs [30]. Recently, a group has demonstrated that MSC-derived ECM can be generated from a patient's own cells ex vivo and such autologous cell-derived ECM does not cause donor site morbidity and host immune response [31].

In this study, we investigated the effects of human dermal fibroblast-derived ECM (hECM) on regulating hMSC stemness and differentiation. We cultured hMSCs with or without hECM and then analyzed cell proliferation, surface antigen expression, and multilineage differentiation.

Materials and Methods

Isolation and Expansion of hMSCs

Femoral head was obtained from a 53-year-old patient undergoing hip surgery. Ethical approval of human tissue procurement for this study was granted by the Institutional Review Board (IRB) at the University of Wisconsin-Madison. Briefly, bone marrow was harvested from the interior compartment of femoral head and washed with 30 ml of Dulbecco's modified Eagle medium (DMEM; Gibco, Carlsbad, CA, USA). The bone fragment and other tissue were filtered out using a syringe. After centrifugation at 1000 rpm for 5 min, cell pellet was collected and resuspended in 25 ml of HBSS (Invitrogen, Carlsbad, CA, USA) and then slowly added into 20 ml of Ficoll-Paque (GE Health, Pittsburgh, PA, USA), followed by centrifugation at 600*g* for 30 min. Mononuclear cells were separated and plated in 75-cm^2 cell culture flasks after additional washing. Cells were maintained in low-glucose DMEM supplemented with 10 % fetal bovine serum and 1 % antibiotics under 5 % CO_2 at 37 °C. Culture medium was changed every 3 days. Upon 80 % confluence, cells were passaged using 0.05 % trypsin/EDTA (Corning, New York, NY, USA) and re-plated at a cell seeding density of 1000 cells/cm^2. Cells between passages 2 and 5 were used in this study. Details of the experimental setup for each assay are described in Fig. 1.

Preparation of hECM

Neonatal human fibroblasts were isolated from dermal surgical discards obtained from routine circumcision with full written consent. Donor suitability was determined by medical evaluation and clinical testing of blood serum for the presence of pathogens from the donor and the donor's mother. Fibroblast cells were extracted from donor tissue using 2.5 U/mL dispase (Worthington Biochemical, Lakewood, NJ, USA) to first separate the epidermis from dermis, followed by incubation with 378 U/mL of collagenase NB (Nordmark, Uetersen, Germany) for approximately 30 min at 37 °C to digest noncellular dermal tissue for recovery of the target cells. Following enzymatic digestion, the cells were separated from the undigested material using a 500 μm filter and cultured in monolayer using DMEM (Invitrogen, Carlsbad, CA, USA) supplemented with 10 % fetal bovine serum (SeraCare Life Sciences, Milford, MA, USA) and 1 % L-glutamine (Invitrogen, Carlsbad, CA, USA) under 5 % CO_2 at 37 °C. The isolated fibroblasts were expanded to obtain a sufficient number of cells to establish a Master Cell Bank which was tested for all known pathogens and virus as established by CBER's *Points to Consider* [32, 33].

The fibroblasts were cultured on dextran microcarrier beads (G.E. Healthcare Life Sciences, Marlborough, MA, USA) under hypoxic conditions (3–5 % O_2) in a 10-liter working volume, closed-system production bioreactor (Applikon Biotechnology, Delft, The Netherlands). The cells were grown in a proprietary serum-free cell culture medium consisting of DMEM (Hyclone, Logan, UT, USA) supplemented with rice-derived recombinant human serum albumin (Healthgen Biotechnology Corp., Wuhan, China) for up to 3 months as described in a previous report [34]. At the end of the culture period, the cell culture medium was drained out of the bioreactor and insoluble materials consisting of microcarrier beads,

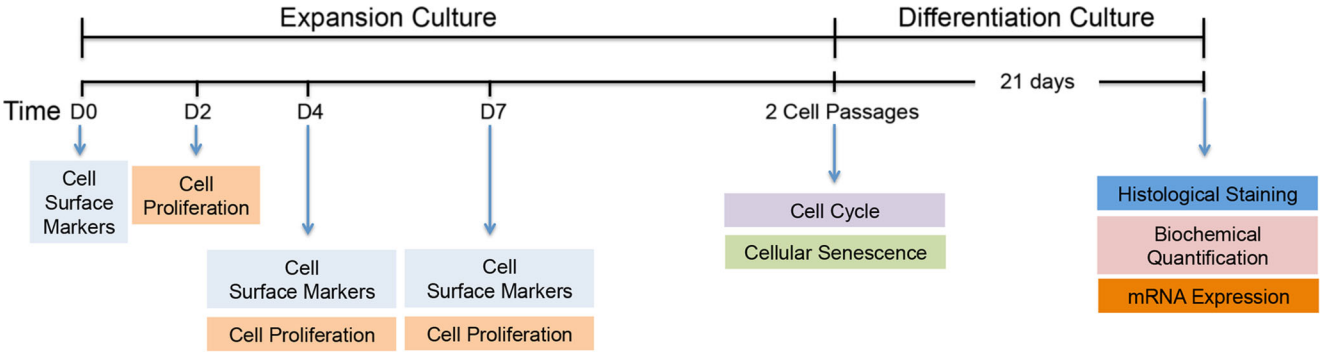

Fig. 1 Timeline of experimental setup

cells and deposited ECM was collected, washed in sterile distilled water, and frozen at −80 °C.

To produce the hECM material for experiments, the frozen material was thawed and washed several times in sterile PBS (Gibco, Grand Island, NY, USA). The material was resuspended in PBS, homogenized using a handheld homogenizer (Polytron Kinematica, Luzern, Switzerland) and incubated with sterile-filtered dextranase (Sigma-Aldrich, St. Louis, MO, USA) at 37 °C to digest the microcarrier beads. The solution was then extensively washed with PBS to generate hECM with a paste-like consistency. The final material was stored at 4 °C until further use. To coat cell culture plates, the hECM material was diluted in PBS at the ratio of 1:10 before being incubated within culture wells overnight at 4 °C.

Characterization of hECM

The hECM material was biochemically characterized by measuring the content of collagen and sulfated glycosaminoglycan (sGAG). Briefly, the hECM slurry was frozen at −80 °C and lyophilized in the FreeZone 4.5 Liter benchtop freeze dry system (LabConco, Kansas City MO) for collagen and sGAG quantification. The hydroxyproline content of the hECM was determined by first dissolving 10 mg of lyophilized material in 0.5 mL of 6 N HCl and heating the samples overnight at 115 °C. The samples were then neutralized to pH 7–8 with 1 N NaOH, and 0.5 mL of each sample was oxidized with 0.25 mL of Chloramine-T solution for 20 min at room temperature, followed by the addition of 0.25 mL of 3.15 M perchloric acid solution and then 0.25 mL of p-dimethylaminobenzaldehyde (pDAB) at 60 °C for 20 min. The amount of 200 uL of the solution was added to each well of a 96-well microtiter plate and measured for colorimetric change at the absorbance wavelength of 561 nm using the SpectraMax M3 plate reader (Molecular Devices, Sunnyvale, CA). Spectrophotometric values of samples were fitted to a curve of 4-hydroxy-L-proline standards to calculate the content of collagen [35] in the dried hECM sample.

Quantification of the sGAG content was performed by enzymatically digesting 5 mg of lyophilized hECM sample overnight at 60 °C in 1.0 mL of 1 mg/mL papain digestion solution containing 0.1 M sodium phosphate, 10 mM EDTA solution, and 5 mM cysteine solution at pH 6.5. Digested samples were briefly centrifuged before 50 uL of the sample was added in a microtiter well to react with 200 uL of dimethylmethylene blue (DMMB) for colorimetric measurement at the absorbance wavelength of 525 nm using the SpectraMax M3 plate reader (Molecular Devices, Sunnyvale, CA). Spectrophotometric values of sGAG samples were fitted to a curve of chondroitin sulfate standards to determine the content of sGAG in the dried hECM sample. All chemicals for hydroxyproline and sGAG assays were obtained from Sigma-Aldrich (St. Louis, MO).

In this study, 5 batches of hECM were characterized by quantifying collagen and sGAG content. To evaluate effects of hECM on regulation of hMSC activities, 2 of the 5 hECM batches were used separately to culture hMSCs.

Analysis of Cell Proliferation

Human MSCs maintained with or without hECM were harvested after 1, 4 and 7 days of culture. Lysis buffer (0.2 % Triton X-100, 10 mM Tris-HCl, and 1 mM EDTA) was used to extract DNA. The total amount of double-stranded DNA (dsDNA) was quantified to determine cell proliferation using the Quant-iT PicoGreen dsDNA assay (Invitrogen) following the manufacturer's instructions. The number of population doublings (PDs) was calculated based on the formula PD=ln(C1/C0)/ln(2), in which C0 equals the initial number of seeded cells and C1 equals the number of cells at the time of measurement.

Analysis of Cell Surface Markers

The expression of cell surface markers was analyzed by flow cytometry. Briefly, hMSCs cultured with or without hECM were harvested at days 0, 4, and 7 and washed with an ice-cold PBS buffer containing 1 % bovine serum albumin and 0.1 % sodium azide (Sigma-Aldrich, St. Louis, MO). The cells were then incubated with PE-conjugated anti-CD73 antibody,

APC-conjugated anti-CD90 antibody, FITC-conjugated anti-CD105 antibody, and PerCP-conjugated anti-CD45 antibody (BD Bioscience, Franklin Lakes, NJ, USA) at 4 °C for 30 min. Cells were then washed three times to remove unbound antibodies and analyzed using flow cytometry with the Flow Jo software to determine the expression of cell surface markers.

Analysis of Cell Cycle

Cell cycle distribution was analyzed by measuring DNA content using propidium iodide (PI) staining. Briefly, 1×10^6 hMSCs maintained with or without hECM were harvested after two cell passages and fixed with 70 % ethanol at 4 °C overnight. Cells were then collected and washed with PBS, followed by an incubation with PI/RNase staining buffer (BD Bioscience) overnight at 4 °C before flow cytometric analysis. Cell cycle data were modeled using the ModFit software.

Analysis of Cellular Senescence

The activity of senescence-associated β-galactosidase was detected by a commercially available staining kit (Cell Signaling Technology, Danvers, MA, USA). Briefly, after maintained with or without hECM for two cell passages, hMSCs were treated with fixative solution containing 2 % formaldehyde and 0.2 % glutaraldehyde for 10 min at room temperature, rinsed twice with PBS, and incubated with staining solution composed of 40 mM citric acid/sodium phosphate, 150 mM NaCl, 2 mM $MgCl_2$, 50 mM potassium ferrocyanide, and 50 mM potassium ferricyanide at pH 6.0 for 16 h at 37 °C. The percentage of cells stained positive for β-galactosidase was determined.

Total RNA Isolation and Quantitative Reverse Transcription-Polymerase Chain Reaction (RT-PCR)

Total RNA was extracted using the Nucleo Spin RNA II kit (Clontech, Mountain View, CA, USA) following the manufacturer's instructions. The amount of 100 ng RNA was then converted into complementary DNA using the High-Capacity cDNA Reverse Transcription kit (Applied Biosystems, Carlsbad, CA, USA). Quantitative PCR was performed using the iQ SYBR Green Supermix (BioRad, Hercules, CA) with the primers listed in Table 1. Relative mRNA levels of target genes were determined using the ΔΔCT method with ubiquitin C (UBC) as an internal reference.

Assessment of Multilineage Differentiation of hMSCs

To investigate whether hECM can prime the capability of undifferentiated hMSCs for multilineage differentiation, hMSCs were maintained in culture with or without hECM for two passages and then induced for osteogenesis, adipogenesis, and chondrogenesis without hECM for 21 days.

For osteogenesis, hMSCs at a seeding density of 5000 cells/cm^2 were induced in osteogenic medium composed of low-glucose DMEM, 10 % FBS, 10 mM β -glycerophosphate, 50 μg/ml L-ascorbic acid-2-phosphate, 0.1 μM dexamethasone (Sigma-Aldrich), and antibiotics. To analyze osteogenic differentiation of hMSCs, alkaline phosphatase (ALP) activity was detected using the ALP staining kit (Sigma-Aldrich) after 10 days of induction. To quantify ALP activity, the cells were first lysed with a digestion buffer containing 2 % Triton X-100, 0.15 mM Tris base, 0.1 mM $ZnCl_2$, 0.1 mM $MgCl_2$•$6H_2O$ at pH 9.0 for 1 h at 37 °C and then overnight at 4 °C. The digestion buffer was then analyzed by measuring the reaction kinetics with p-nitrophenyl phosphate (Sigma-Aldrich). The results were normalized to the double-stranded DNA (dsDNA) content that was separately determined by the PicoGreen assay (Invitrogen). At day 21, cells were fixed with 60 % isopropanol and then stained for Alizarin red (Rowley Biochemical, Danvers, MA, USA) to evaluate the extent of mineral deposition. To quantify the level of mineralization, calcium deposition in culture was extracted using 0.5 M hydrogen chloride, and then measured using the LiquiColor kit (Stanbio, Boerne, TX, USA) following the manufacturer' s protocol.

For adipogenesis, hMSCs were plated at a seeding density of 10,000 cells/cm^2 and exposed to adipogenic medium consisting of high glucose DMEM, 10 % FBS, 1 mM dexamethasone, 0.5 mM 3-isobutyl-1-methylxanthine, 1 mg/mL insulin (Sigma-Aldrich), and antibiotics. To evaluate adipogenic differentiation of hMSCs, lipid droplets were visualized using Oil red O (Sigma) after 21 days of induction. The stain was subsequently extracted and measured at the absorbance wavelength of 656 nm to determine the amount of lipid droplets.

For chondrogenesis, the number of 2.5×10^5 hMSCs was centrifuged at 600*g* for 5 min and cultured overnight to form a cell pellet, followed by the induction in serum-free chondrogenic medium composed of DMEM with 4.5 g/L glucose (DMEM-HG; Gibco) supplemented with 1 % antibiotics, 1 % ITS. Premix (BD Biosciences), 0.9 % sodium pyruvate (Sigma), 50 mg/ml ascorbic acid, 40 mg/mL L-proline, 10 ng/ml transforming growth factor beta-1 (TGFB1) (Peprotech Rocky Hill, NJ, USA), and 10^{-7} M dexamethasone. After 21 days of induction, pellets were harvested and fixed with 4 % formaldehyde solution, followed by paraffin embedding and sectioning for histology. Sections were deparaffinized in xylene, hydrated, and then stained by Alcian blue (Polysciences, Warrington, PA, USA) to detect sulfated-glycosaminoglycan (sGAG). Hematoxylin and eosin (H&E) staining was performed to exam the distribution and morphology of hMSCs in cell pellets. For immunolocalization, pellets were first blocked with 0.1 % (wt/vol) BSA in PBS for 20 min and then incubated with the primary antibody against collagen type 1 (C-18; sc-8786), collagen type 2

Table 1 Primer sequences for quantitative RT-PCR analysis

Gene name	Accession number	Primer sequences (5′ to 3′)
UBC	NM_021009.4	F:TGAAGACACTCACTGGCAAGACCA
		R:CAGCTGCTTTCCGGCAAAGATCAA
OCT3/4	NM_002701.4	F:TGGAGAAGGAGAAGCTGGAGCAAAA
		R: GGCAGATGGTCGTTTGGCTGAATA
NANOG	NM_021865.2	F:GCTGAGATGCCTCACACGGAG
		R:TCTGTTTCTTGACCGGGACCTTGTC
SOX2	NM_003106.2	F:GGGAAATGGGAGGGGTGCAAAAGAGG
		R:TTGCGTGAGTGTGGATGGGATTGGTG
SOX9	NM_000346.3	F:TAAAGGCAACTCGTACCCAA
		R:ATTCTCCATCATCCTCCACG
RUNX2	NM_004348.3	F:GGTTCCAGCAGGTAGATGAG
		R:AGACACCAAACTCCACAGCC
PPARG	NM_138711.3	F:ATGACAGCGACTTGGCAATA
		R:GGCTTGTAGCAGGTTGTCTTG
ALP	NM_000478.3	F:CAAAGGCTTCTTCTTGCTGG
		R:GGTCAGAGTGTCTTCCGAGG
OC	NM_199173.3	F:GACTGTGACGAGTTGGCTAGA
		R:GGAAGAGGAAAGAAGGGTGC
LPL	NM_000237.2	F:AGGAGCATTACCCAGTGTCC
		R:GGCTGTATCCCAAGAGATGGA
AGN	NM_013227.2	F:CACGATGCCTTTCACCACGAC
		R:TGCGGGTCAACAGTGCCTATC
COL2	NM_001844.4	F:CCTCTGCGACGACATAATCT
		R:CTCCTTTCTGTCCCTTTGGT
p21	NM_078467.1	F: GCGGCAGGCGCCATGTCAGA
		R: CCTGGATGCAGCCCGCCATT
p16	NM_000077.3	F: AGCCTTCGGCTGACTGGCTGG
		R: CCATCATCATGACCTGGATCG

Forward and reverse primers are indicated as "F" and "R", respectively

(N-19; sc-7764), and collagen type 10 (E-14; sc-323750) (Santa Cruz Biotechnology, Santa Cruz, CA) overnight at 4 °C. The sections were then washed three times with PBS followed by the incubation with second antibody (donkey anti-goat-FITC, 1:100, Santa Cruz Biotechnology) for 45 min. After three additional washings, sections were stained with DAPI. To quantify the sGAG amount in pellets, samples were first digested by papain for 24 h at 60 °C. Total sGAG was quantified using the Blyscan Assay kit (Biocolor, Westbury, NY, USA) following the manufacturer's protocol and then normalized to total DNA content using the Quant-iT PicoGreen dsDNA Assay kit (Invitrogen).

Statistical Analysis

All quantitative assays were performed in triplicate. Data were expressed as the mean ± SD and Student's *t*-test was performed to determine levels of statistical significance. A p-value < 0.05 was considered significant.

Results

Fibroblast-Derived ECM Regulates hMSCs Behavior

Five different batches of hECM were characterized to determine whether there was variation in composition between batches of the material. The results showed similar ratios of the dry weight of collagen or sGAG content to hECM between the 5 batches of samples (Fig. 2), indicating that hECM with consistent batch-to-batch collagen and sGAG content was used in this study.

To test whether hECM derived from fibroblasts can stimulate the proliferation of hMSCs, we cultured hMSCs with or without hECM for 7 days before analysis. Our results showed that cells maintained in the culture with and without hECM for 7 days showed similar cell morphology (Fig. 3a). The DNA content in the hECM-treated culture was significantly higher than that in the control culture on days 4 and 7, suggesting that hECM is able to increase the number of hMSCs in culture (Fig. 3b). After

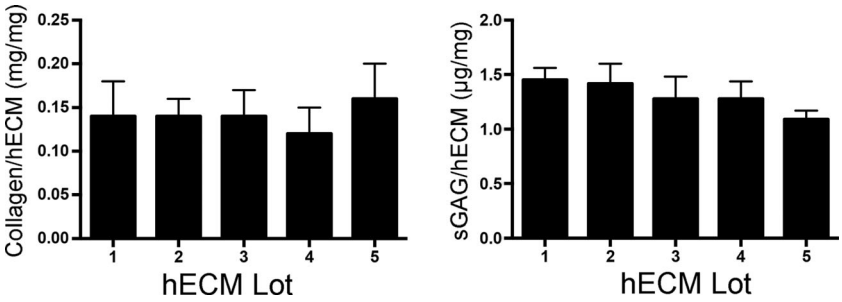

Fig. 2 Quantification of collagen and sGAG content in dried hECM. Amounts of collagen and sGAG in hECM of 5 different batches were individually determined

calculation, the results showed that hMSCs in hECM culture underwent more accumulated PDs than control cells (Fig. 3c). Analysis of cell surface markers was performed to determine the amount of the $CD73^+/CD90^+/CD105^+/CD45^-$ subpopulation in heterogeneous hMSCs as recommended by the International Society for Cellular Therapy [36]. The subpopulation in hMSCs cultured with hECM at day 0, 4, or 7 of culture identified by flow cytometry was 78.6 %, 53.2 %, or 87.1 %, respectively while that in control hMSCs was 78.6 %, 92.5 %, or 97.7 %, respectively (Fig. 3d). However, it should be noted that the amount of total hMSCs determined by DNA content in hECM culture at day 4 or 7 was 2.28 or 1.6 times, respectively, more than that in control culture. Calculated based on the data of amount of total hMSCs and percentage of the subpopulation, the $CD73^+/CD90^+/CD105^+/CD45^-$ subpopulation in hECM culture was about 2.4-fold at day 4 and 9.5-fold at day 7 greater than that at day 0 while in control culture without hECM, the $CD73^+/CD90^+/CD105^+/CD45^-$ subpopulation was increased only about 2.1-fold at day 4 and 7.3-fold at day 7 compared to that at day 0 (Fig. 3d). These results suggest that hECM is capable of increasing the $CD73^+/CD90^+/CD105^+/CD45^-$ hMSC subpopulation during expansion culture.

We analyzed cell cycle distribution of hMSCs regulated by hECM using flow cytometry and the result showed that 21 % of hMSCs cultured with hECM was in S phase compared to 12 % of the cell maintained in culture without hECM (Fig. 4a). The result suggests that hECM arrests fewer hMSCs in G0/G1 phase but facilitates the cell to enter into S phase, which resulted in increased cell proliferation. We also analyzed cellular senescence of hMSCs treated with or without hECM. The mRNA expression levels of senescence-associated markers, *p21 and p16*, between hMSCs cultured with and without hECM were comparable. In addition, we detected the activity of β-galactosidase to further analyze cellular senescence. The result of β-galactosidase staining showed that the percentage of hMSCs stained positive for β-galactosidase activity in hECM culture was similar to that in control culture without hECM (Fig. 4b), suggesting that hECM does not induce cellular senescence of cultured hMSCs.

We next investigated the effect of hECM on regulating the potential of multilineage differentiation of hMSCs. RT-PCR analysis showed that the mRNA expression of potency-related markers, *OCT3/4, NANOG, SOX2*, was comparable between hMSCs in culture with or without hECM (Fig. 5). However, the mRNA expression of lineage-specific markers showed that hECM did not affect the expression level of the osteogenic transcriptional factor, *CBFA1*, but significantly increased the expression level of adipogenic and chondrogenic transcriptional factors, *PPARG* and *SOX9*, respectively (Fig. 5). These results together with those of Fig. 3d suggest that ECM derived from human dermal fibroblasts may have the capacity to drive hMSCs toward adipogenesis and chondrogenesis.

Fibroblast-Produced ECM Directs Lineage-Specific Differentiation of hMSCs

To determine whether hECM directs hMSCs to undergo lineage-specific differentiation, hMSCs maintained in culture with or without hECM for two passages were then induced into the osteogenic, chondrogenic, or adipogenic lineage without hECM. After 21 days of osteogenesis, the mRNA expression of *CBFA1* or *ALP* in ECM-pretreated hMSCs was comparable to that in control hMSCs without being precultured with hECM while the mRNA expression of *OC* was significantly downregulated in hMSCs pretreated with hECM (Fig. 6a). Consistently, on day 10, the results of ALP staining and quantification showed similar levels of ALP activity between hMSCs with and without hECM treatment (Fig. 6b). However, calcium deposition after 21 days of osteogenic induction showed a significant decrease in hMSCs precultured with hECM compared to those precultured without hECM (Fig. 6c). Our findings indicate that fibroblast-produced ECM may reduce osteogenic differentiation of hMSCs. We next evaluated the effect of hECM on adipogenic differentiation of hMSCs.

The results of quantitative RT-PCR showed no significant difference in the mRNA levels of *LPL* and *PPARG* between hMSCs pretreated with and without hECM (Fig. 7a). Nonetheless, there were significantly less lipid droplets stained by Oil red O produced by hMSCs precultured with hECM than those by control cells precultured without hECM after 21 days of induction (Fig. 7b). These results suggest that hECM also reduces adipogenic differentiation of hMSCs.

Human MSCs pretreated with or without hECM were made into high-density cell pellets and induced for chondrogenesis for 21 days. Our results showed that hECM pretreatment significantly upregulated the mRNA expression levels of *COL2*,

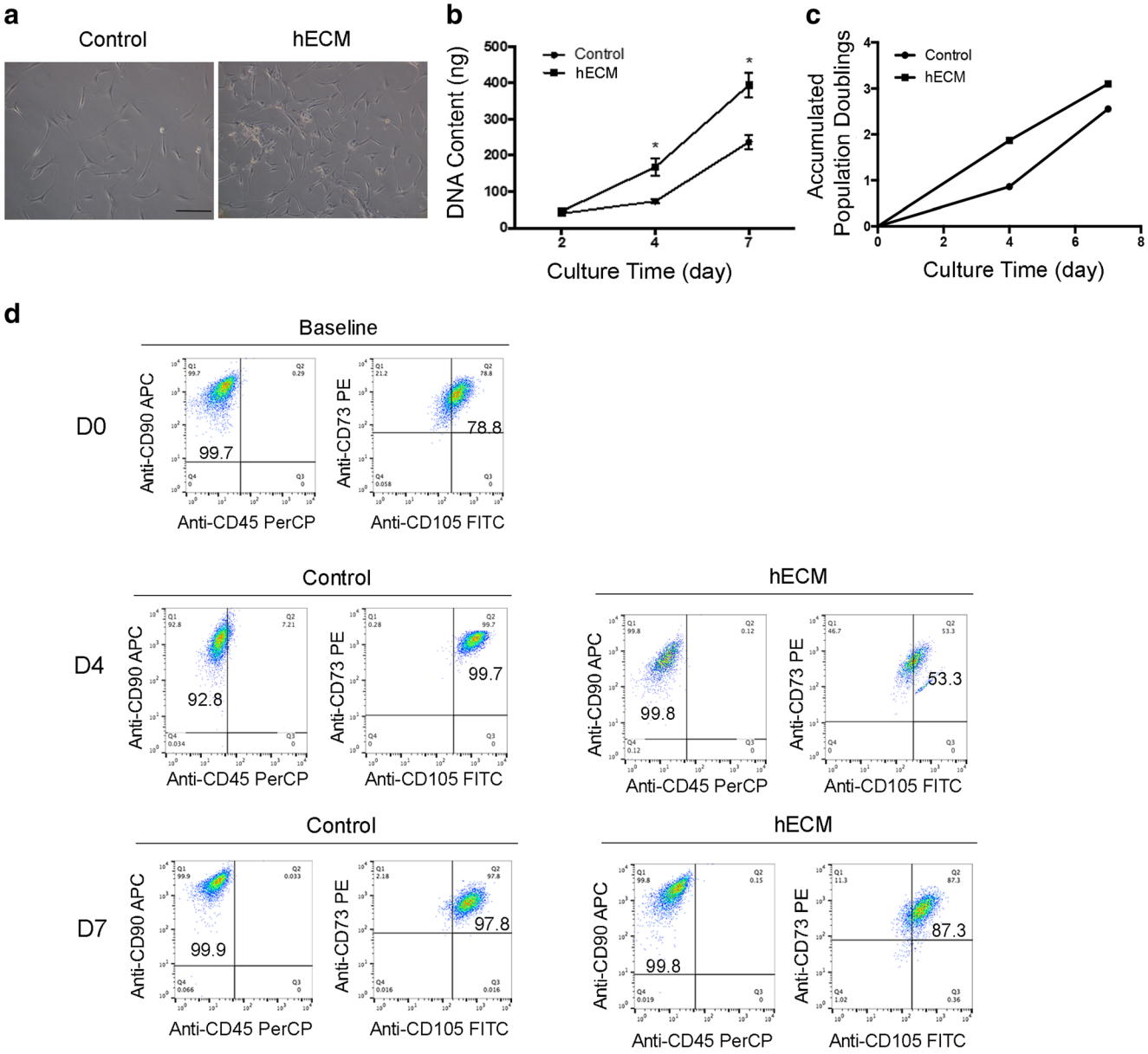

		Subpopulation (%)	Total hMSC Amount (in DNA content)	Subpopulation Amount (in DNA content)
D0	Control	99.7 x 78.8 = 78.56	40.2	78.56% x 40.2 = 31.58
	hECM	99.7 x 78.8 = 78.56	45.9	78.56% x 45.9 = 36.06
D4	Control	92.8 x 99.7 = 92.52	73.2	92.52% x 73.2 = 67.72
	hECM	99.8 x 53.3 = 53.19	167.6	53.19% x 167.6 = 87.47
D7	Control	99.9 X 97.8 = 97.70	236.7	97.70% x 236.7 = 231.26
	hECM	99.8 X 87.3 = 87.12	393.9	87.12% x 393.9 = 343.17

Fig. 3 Effects of hECM on regulation of proliferation and expression of surface markers of hMSCs. **a** Cell morphology of hMSCs maintained with or without hECM for 7 days. Scale bar: 200 μm. **b** Proliferation of hMSCs cultured with or without hECM was analyzed by quantifying total DNA content. **c** Accumulated population doublings of hMSCs in short-term culture with or without hECM. **d** The percentage of the $CD90^+/CD105^+/CD73^+/CD45^-$ subpopulation on day 0 as a baseline or in culture with or without hECM for 4 and 7 days was determined. Each data set of flow cytometry analysis was collected from 10,000 cells. Percentage of the subpopulation, total hMSC amount, and subpopulation amount were calculated and summarized in the table

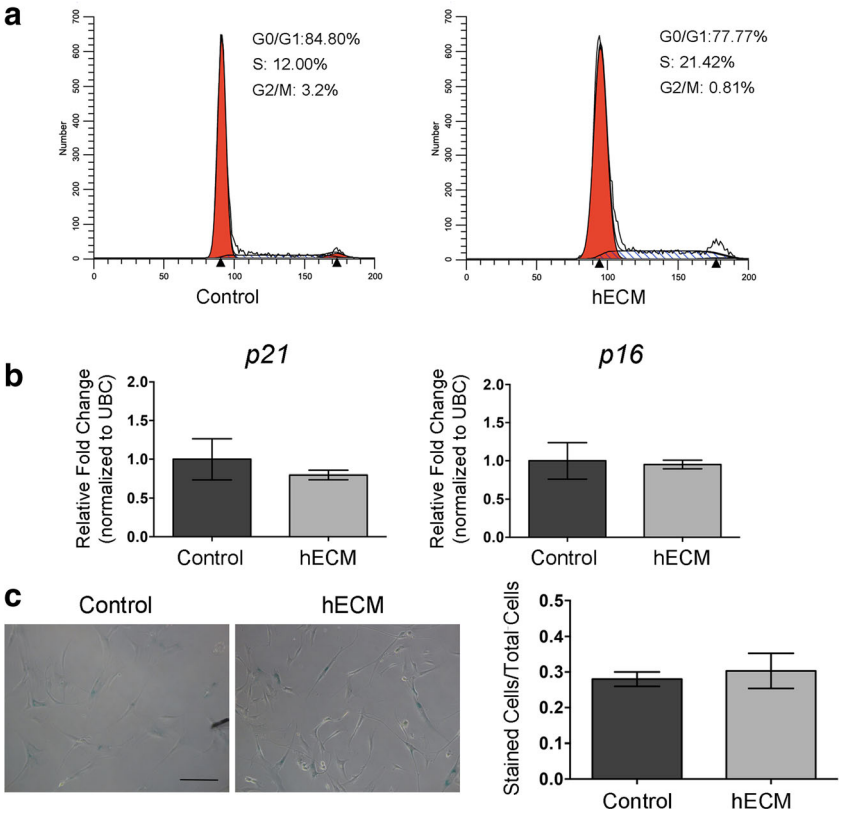

Fig. 4 Effects of hECM on regulation of cell cycle distribution and cellular senescence. **a** Cell cycle distribution analyzed by flow cytometry to detect propidium iodide staining. Percentages of cells in different phases were determined based on DNA content. **b** Relative mRNA expression levels of senescence-related markers analyzed by quantitative RT-PCR. **c** Staining and quantification of β-galactosidase activity in hMSCs cultured with or without hECM. Scale bar: 200 μm

AGN, and *SOX9* in hMSCs compared to those in control cells (Fig. 8a). Histological analysis showed similar intensity levels of Alcian blue staining between cell pellets of ECM-pretreated and control hMSCs (Fig. 8b). The GAG quantification assay also showed that cell pellets of hMSCs pretreated with hECM produced similar amounts of GAGs compared to control hMSCs without being pretreated with hECM (Fig. 8b). However, H&E and Alcian blue staining showed that a larger region rich in protein matrix and GAGs was found around the edge of cell pellets made of hECM-pretreated hMSCs than that in cell pellets of control hMSCs, indicating that hECM-pretreated hMSCs produced more cartilaginous matrix during chondrogenic differentiation (Fig. 8b).

To localize COL1, COL2, and COL10, immunofluorescent staining was performed after 21 days of chondrogenic induction. We found that less COL1 expressed in cell pellets of

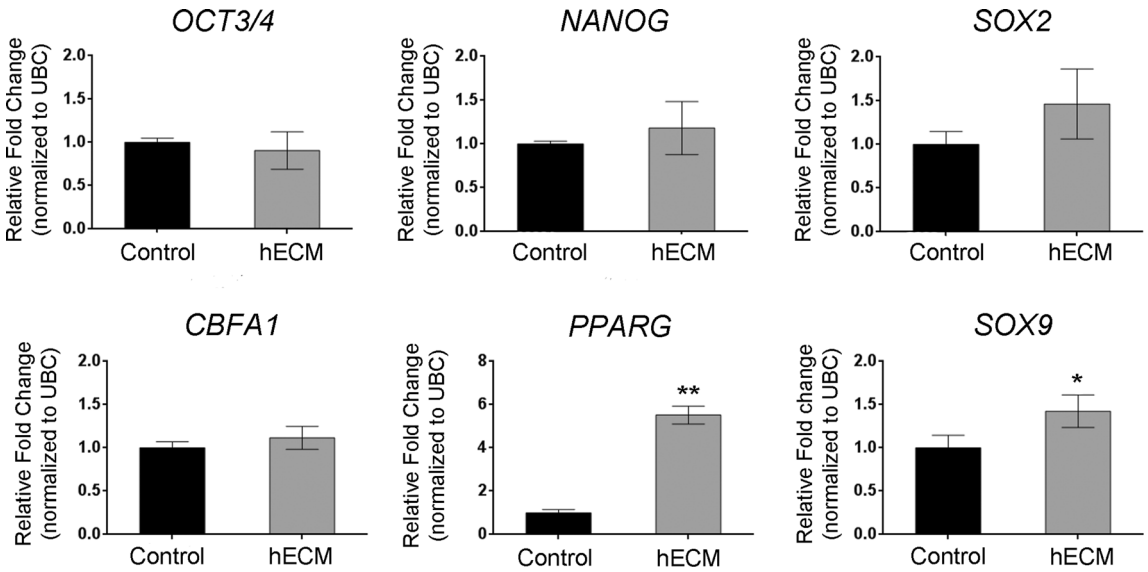

Fig. 5 Effects of hECM on the mRNA expression of potency-related and lineage-specific markers in pre-differentiated hMSCs. *$p < 0.05$; **$p < 0.01$; $n = 3$

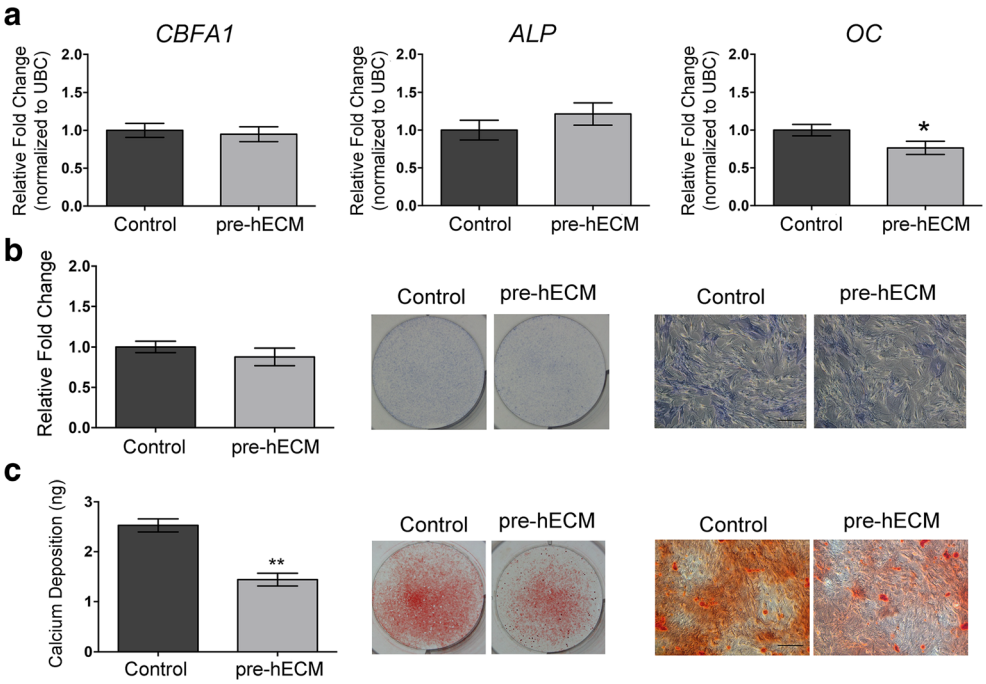

Fig. 6 Osteogenic differentiation of hMSCs pre-treated with or without hECM. **a** Relative mRNA expression levels of bone-related markers were analyzed by quantitative RT-PCR. **b** Analysis of ALP staining and quantification was performed to determine hMSCs osteogenesis. **c** Calcium deposition was detected by Alizarin red staining and quantified to determine hMSCs osteogenesis. *$p < 0.05$; **$p < 0.01$; $n = 3$. Scale bar: 200 μm

hECM-pretreated hMSCs than in cell pellets of control cells. Conversely, cell pellets of hECM-pretreated hMSCs showed much more COL2 and COL10 production compared to those of control hMSCs. These findings suggest that hECM upregulates the chondrogenic capacity of pre-differentiated hMSCs, which in turn leads to increased chondrogenesis upon receiving differentiation induction (Fig. 8c).

Discussion

In this study, we have demonstrated that hECM upregulates hMSC proliferation, increases the amount of $CD90^+/CD105^+/CD73^+/CD45^-$ subpopulation, and primes hMSCs for chondrogenic differentiation while downregulating their osteogenic and adipogenic capacity.

ECM plays an important role in tissue structure maintenance and cell fate determination. It has been shown that compared to MSCs cultured on either fibronectin-, collagen type 1- or collagen type 2-coated plate, the cell grown on cell-derived ECM expresses higher levels of osteogenic markers [37], suggesting that ECM provides more comprehensive regulation on cellular activity then single-ECM proteins. Our results have also shown that compared to fibronectin, a potent adhesion molecule, cell-derived ECM is capable of increasingly inducing proliferation of hMSCs (Supplementary data). The difference in ECM components among various tissues can regulate

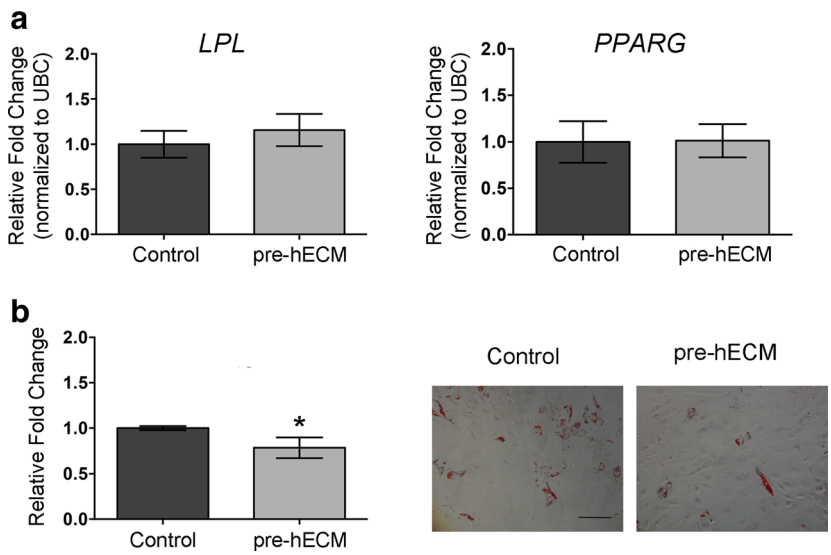

Fig. 7 Adipogenic differentiation of hMSCs pre-treated with or without hECM. **a** Relative mRNA expression levels of adipose-related markers were analyzed by quantitative RT-PCR. **b** The production of lipid droplets was quantified and detected by Oil Red O staining. *$p < 0.05$; $n = 3$. Scale bar: 200 μm

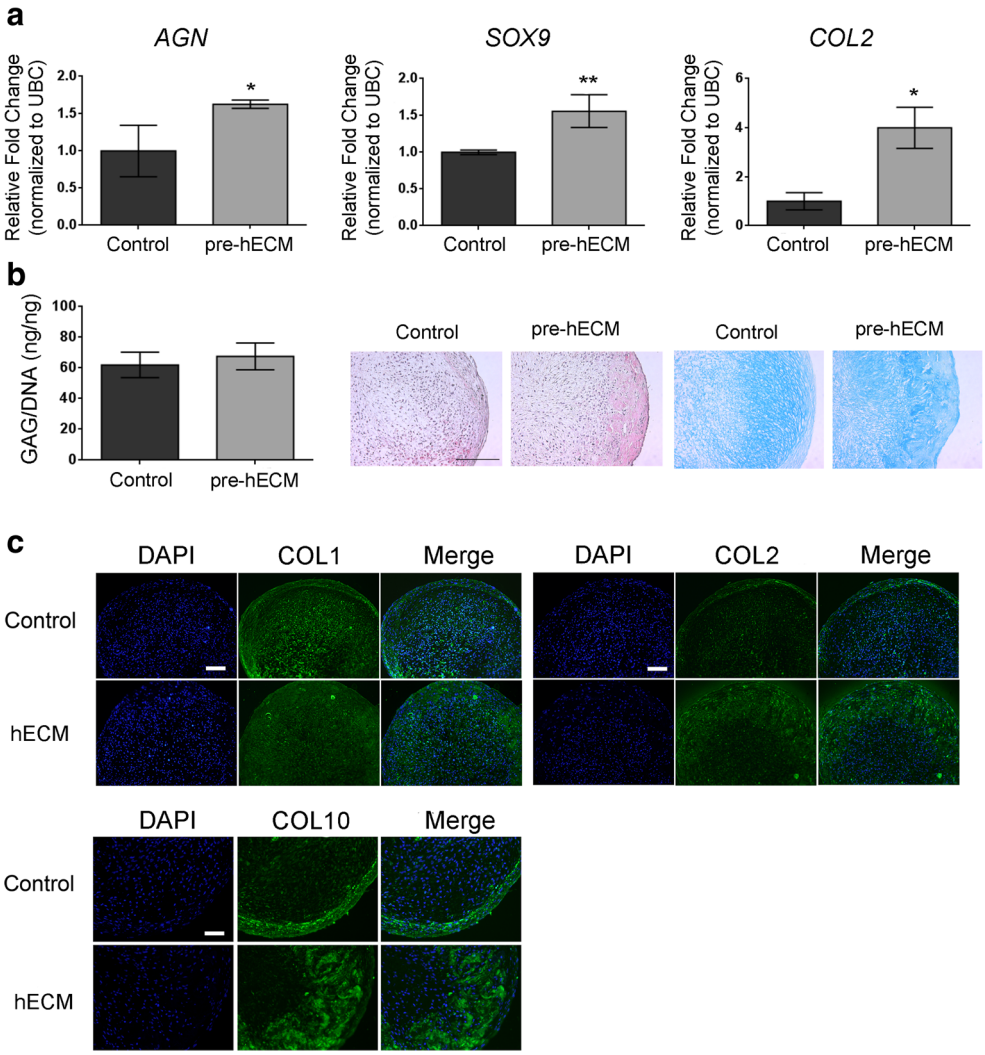

Fig. 8 Chondrogenic differentiation of hMSCs pre-treated with or without hECM. **a** Relative mRNA expression levels of cartilage-related markers were analyzed by quantitative RT-PCR. **b** GAG quantification, H&E staining, and Alcian blue staining were performed to assess chondrogenesis of hMSCs. **c** Localization of COL1, COL2 and COL10 by immunofluorescent staining $*p < 0.05$; $**p < 0.01$; $n = 3$. Scale bar: 200 μm

cell behavior differently. Rao et al. and Kwon et al. have compared the modulation of MSC proliferation and differentiation by different cell-derived ECM and found that ECM produced by undifferentiated MSCs enhances cell proliferation while maintaining stemness of the cell [37, 38]. Moreover, they have shown that MSCs cultured on osteogenic hMSC- or osteoblast-derived ECM are directed toward osteoblasts while MSCs on chondrocyte- or smooth muscle cell-derived ECM are induced into chondrocyte or smooth muscle cell, respectively. Rao et al. have also shown that the osteoinductive potential of ECM produced by osteogenic hMSCs in early differentiation stage is greater than that in late differentiation stage, indicating that the ECM compositions at distinct differentiation stages are different [38].

Human dermal fibroblasts are extensively used as feeder cells in the hESC culture system to support hESC growth and maintain the pluripotency in vitro [39–41]. A recent study has demonstrated that ECM produced by human dermal fibroblasts is able to support long-term culture of hESCs [42]. These findings together suggest that human dermal fibroblasts are potent to the regulation of cell properties ex vivo. In this study, we culture hMSCs on hECM-coated substrates before induction for multilineage differentiation to investigate whether hECM is able to modulate the phenotype and differentiation potential of hMSCs. We have found that hMSCs treated with hECM increasingly proliferate compared to those without hECM exposure while no differences in regulation of cellular senescence between hMSCs cultured with and without hECM were found. More of $CD90^{+}/CD105^{+}/CD73^{+}/CD45^{-}$ cells are retrieved from the whole MSC population maintained on hECM than on the control surface without hECM coating. Moreover, hMSCs pre-cultured with hECM show increased chondrogenic potential compared to control MSCs. On the other hand, the capacity of osteogenesis is downregulated by hECM pretreatment. Interestingly, the upregulated mRNA expression level of *PPARG* in hMSCs by hECM before adipogenic induction does not result in increased adipogenesis, suggesting that

the adipogenic capacity enhanced by hECM is only at the transcriptional level.

For MSC-based therapies, a large quantity of MSCs is needed for disease treatment. A previous study has suggested that single or multiple doses of approximately 2×10^6 cells per kilogram of the body weight is required for effective treatment [43]. For tissue engineering, the capacity to produce a large amount of MSCs in a relatively short period of time is also required. Thus, developing an approach that can effectively expand MSCs in vitro is critical for MSC-based tissue engineering and regeneration. Our results have shown that hECM capable of increasing hMSC proliferation can be used for ex vivo hMSC expansion.

Mesenchymal stem cells contain heterogeneous cell populations [44]. International Society for Cell Therapy has recommended that the minimum criteria that identify MSCs are the cell should be positive for CD105, CD73, and CD90 but negative for CD45, CD34, CD14 or CD11b, CD79a or CD19, and HLA-DR [36]. Kawamoto et al. have demonstrated that the population of $CD90^{high}$ MSCs derived from murine adipose tissue has a greater reprograming capacity compared to the unsorted population [45]. Moreover, the $CD105^+$ population in synovium-derived MSCs has been shown to be more proliferative and chondrogenic than the whole MSC population [46]. These findings suggest that a MSC subpopulation composed of $CD105^+$, $CD73^+$ and $CD90^+$ cells may have a greater therapeutic capacity than the whole MSC population. Our results show that culturing hMSCs with hECM capable of increasing the $CD90^+/CD105^+/CD73^+/CD45^-$ subpopulation is a viable strategy to enhance the therapeutic potential of hMSCs.

Collagen molecules, including collagen types 2, 6, 9, 10, and 11, are found in adult articular cartilage [47]. Collagen type 2 constituting approximately 95 % of the collagen in articular cartilage is a predominant component responsible for tensile strength [48]. Collagen type 10 primarily located in the calcified cartilage layer is a major protein produced by hypertrophic chondrocytes [49]. Different from collagen types 2 and 10, collagen type 1 is mainly distributed in fibrocartilage. Lu et al. have reported that MSC- and chondrocyte-derived ECM increases the production of collagen types 1 and 2 simultaneously in chondrogenic MSCs [50]. In this study, our immunofluorescent results show that hECM-pretreated MSCs produce more collagen types 2 and 10 but less collagen type 1 than control cells, suggesting that hECM may be well suitable for induction of hyaline cartilage formation. However, since collagen type 10 is a marker of hypertrophic chondrocytes, expressed at the terminal stage of chondrogenesis [51, 52], our future study will focus on de-coupling the expression of collage types 2 and 10.

Conclusion

Our findings demonstrating the effect of hECM on MSC activities with the results showing an increase in proliferation of the $CD90^+/CD105^+/CD73^+/CD45^-$ subpopulation, directing hMSCs toward the chondrogenic lineage, and production of hyaline cartilage markers are important to addressing the current challenges associated with MSC expansion in vitro and cartilage tissue engineering.

Acknowledgments We would like to thank Dr. Matthew Squire for his assistance in providing human femoral heads for MSC isolation. We would also like to thank PUR Biologics for providing funding to support this study. Lastly, we want to thank the University of Wisconsin Carbone Cancer Center supported by the grant P30 CA014520 for the use of its flow cytometry facility.

Compliance with Ethical Standards

Conflict of Interest This study was sponsored by PUR Biologics.

References

1. Loeser, R. F. (2010). Age-related changes in the musculoskeletal system and the development of osteoarthritis. *Clinics in Geriatric Medicine, 26*, 371–386.
2. Collins, J. (2013). Letter from the editor: effects of aging on the musculoskeletal system. *Seminars in Roentgenology, 48*, 105–106.
3. Musumeci, G., Szychlinska, M. A., & Mobasheri, A. (2015). Age-related degeneration of articular cartilage in the pathogenesis of osteoarthritis: molecular markers of senescent chondrocytes. *Histology and Histopathology, 30*, 1–12.
4. Ferrari, S. L. (2005). Osteoporosis: a complex disorder of aging with multiple genetic and environmental determinants. *World Review of Nutrition and Dietetics, 95*, 35–51.
5. Barry, F. P., & Murphy, J. M. (2004). Mesenchymal stem cells: clinical applications and biological characterization. *The International Journal of Biochemistry & Cell Biology, 36*, 568–584.
6. Javazon, E. H., Beggs, K. J., & Flake, A. W. (2004). Mesenchymal stem cells: paradoxes of passaging. *Experimental Hematology, 32*, 414–425.
7. Hanson, S. E., Gutowski, K. A., & Hematti, P. (2010). Clinical applications of mesenchymal stem cells in soft tissue augmentation. *Aesthetic Surgery Journal / the American Society for Aesthetic Plastic Surgery, 30*, 838–842.
8. Kim, N., & Cho, S. G. (2013). Clinical applications of mesenchymal stem cells. *The Korean Journal of Internal Medicine, 28*, 387–402.
9. Shekkeris, A. S., Jaiswal, P. K., & Khan, W. S. (2012). Clinical applications of mesenchymal stem cells in the treatment of fracture non-union and bone defects. *Current Stem Cell Research & Therapy, 7*, 127–133.
10. Miura, Y. (2015). Human bone marrow mesenchymal stromal/stem cells: current clinical applications and potential for hematology. *International Journal of Hematology*. doi:10.1007/s12185-015-1920-z.

11. Grigolo, B., Lisignoli, G., Desando, G., et al. (2009). Osteoarthritis treated with mesenchymal stem cells on hyaluronan-based scaffold in rabbit. *Tissue Engineering. Part C, Methods, 15*, 647–658.
12. Alfaqeh, H., Norhamdan, M. Y., Chua, K. H., Chen, H. C., Aminuddin, B. S., & Ruszymah, B. H. (2008). Cell based therapy for osteoarthritis in a sheep model: gross and histological assessment. *The Medical Journal of Malaysia, 63 Suppl A*, 37–38.
13. Murphy, J. M., Fink, D. J., Hunziker, E. B., & Barry, F. P. (2003). Stem cell therapy in a caprine model of osteoarthritis. *Arthritis and Rheumatism, 48*, 3464–3474.
14. Grayson, W. L., Zhao, F., Bunnell, B., & Ma, T. (2007). Hypoxia enhances proliferation and tissue formation of human mesenchymal stem cells. *Biochemical and Biophysical Research Communications, 358*, 948–953.
15. Palumbo, S., Tsai, T. L., & Li, W. J. (2014). Macrophage migration inhibitory factor regulates AKT signaling in hypoxic culture to modulate senescence of human mesenchymal stem cells. *Stem Cells and Development, 23*, 852–865.
16. Handorf, A. M., & Li, W. J. (2011). Fibroblast growth factor-2 primes human mesenchymal stem cells for enhanced chondrogenesis. *PloS One, 6*, e22887.
17. Lee, J. Y., Zhou, Z., Taub, P. J., et al. (2011). BMP-12 treatment of adult mesenchymal stem cells in vitro augments tendon-like tissue formation and defect repair in vivo. *PloS One, 6*, e17531.
18. Chiu, L. H., Yeh, T. S., Huang, H. M., Leu, S. J., Yang, C. B., & Tsai, Y. H. (2012). Diverse effects of type II collagen on osteogenic and adipogenic differentiation of mesenchymal stem cells. *Journal of Cellular Physiology, 227*, 2412–2420.
19. Rakian, R., Block, T. J., Johnson, S. M., et al. (2015). Native extracellular matrix preserves mesenchymal stem cell "stemness" and differentiation potential under serum-free culture conditions. *Stem Cell Research & Therapy, 6*, 235.
20. Chen, X. D. (2010). Extracellular matrix provides an optimal niche for the maintenance and propagation of mesenchymal stem cells. *Birth Defects Research. Part C, Embryo Today : Reviews, 90*, 45–54.
21. Gattazzo, F., Urciuolo, A., & Bonaldo, P. (2014). Extracellular matrix: a dynamic microenvironment for stem cell niche. *Biochimica et Biophysica Acta, 1840*, 2506–2519.
22. Watt, F. M., & Huck, W. T. (2013). Role of the extracellular matrix in regulating stem cell fate. *Nature Reviews. Molecular Cell Biology, 14*, 467–473.
23. Wei, Q., Pohl, T. L., Seckinger, A., Spatz, J. P., & Cavalcanti-Adam, E. A. (2015). Regulation of integrin and growth factor signaling in biomaterials for osteodifferentiation. *Beilstein Journal of Organic Chemistry, 11*, 773–783.
24. Somers, P., Cornelissen, R., Thierens, H., & Van Nooten, G. (2012). An optimized growth factor cocktail for ovine mesenchymal stem cells. *Growth Factors, 30*, 37–48.
25. Peng, T., Zhu, G., Dong, Y., et al. (2015). BMP4: a possible key factor in differentiation of auditory neuron-like cells from bone-derived mesenchymal stromal cells. *Clinical Laboratory, 61*, 1171–1178.
26. Hughes, C. S., Postovit, L. M., & Lajoie, G. A. (2010). Matrigel: a complex protein mixture required for optimal growth of cell culture. *Proteomics, 10*, 1886–1890.
27. Zheng, Y. L., Sun, Y. P., Zhang, H., et al. (2015). Mesenchymal stem cells obtained from synovial fluid mesenchymal stem cell-derived induced pluripotent stem cells on a Matrigel coating exhibited enhanced proliferation and differentiation potential. *PloS One, 10*, e0144226.
28. Uemura, M., Refaat, M. M., Shinoyama, M., Hayashi, H., Hashimoto, N., & Takahashi, J. (2010). Matrigel supports survival and neuronal differentiation of grafted embryonic stem cell-derived neural precursor cells. *Journal of Neuroscience Research, 88*, 542–551.
29. Ng, C. P., Sharif, A. R., Heath, D. E., et al. (2014). Enhanced ex vivo expansion of adult mesenchymal stem cells by fetal mesenchymal stem cell ECM. *Biomaterials, 35*, 4046–4057.
30. He, H., Liu, X., Peng, L., et al. (2013). Promotion of hepatic differentiation of bone marrow mesenchymal stem cells on decellularized cell-deposited extracellular matrix. *BioMed Research International, 2013*, 406871.
31. Nejadnik, H., Hui, J. H., Feng Choong, E. P., Tai, B. C., & Lee, E. H. (2010). Autologous bone marrow-derived mesenchymal stem cells versus autologous chondrocyte implantation: an observational cohort study. *The American Journal of Sports Medicine, 38*, 1110–1116.
32. Kruse, P. F. Jr, & Patterson, M. K. Jr (Eds) (1973). Tissue culture methods and applications. New York: Academic Press.
33. Administration UFaD. (1993). *Points to consider in the characterization of cell line used to produce biologicals*. Bethesda: US Department of Health and Human Services.
34. Pinney, E., Zimber, M., Schenone, A., Montes-Camacho, M., Ziegler, F., & Naughton, G. K. (2011). Human Embryonic-like ECM (hECM) stimulates proliferation and differentiation in stem cells while killing cancer cells. *International Journal of Stem Cells, 4*, 70–75.
35. Neuman, R. E., & Logan, M. A. (1950). The determination of collagen and elastin in tissues. *The Journal of Biological Chemistry, 186*, 549–556.
36. Dominici, M., Le Blanc, K., Mueller, I., et al. (2006). Minimal criteria for defining multipotent mesenchymal stromal cells. The International Society for Cellular Therapy Position Statement. *Cytotherapy, 8*, 315–317.
37. Kwon, S. H., Lee, T. J., Park, J., et al. (2013). Modulation of BMP-2-induced chondrogenic versus osteogenic differentiation of human mesenchymal stem cells by cell-specific extracellular matrices. *Tissue Engineering Part A, 19*, 49–58.
38. Rao Pattabhi, S., Martinez, J. S., & Keller, T. C., 3rd. (2014). Decellularized ECM effects on human mesenchymal stem cell stemness and differentiation. *Differentiation; Research in Biological Diversity, 88*, 131–143.
39. Anisimov, S. V., Christophersen, N. S., Correia, A. S., et al. (2011). Identification of molecules derived from human fibroblast feeder cells that support the proliferation of human embryonic stem cells. *Cellular & Molecular Biology Letters, 16*, 79–88.
40. Park, Y., Kim, J. H., Lee, S. J., et al. (2011). Human feeder cells can support the undifferentiated growth of human and mouse embryonic stem cells using their own basic fibroblast growth factors. *Stem Cells and Development, 20*, 1901–1910.
41. Unger, C., Gao, S., Cohen, M., et al. (2009). Immortalized human skin fibroblast feeder cells support growth and maintenance of both human embryonic and induced pluripotent stem cells. *Human Reproduction, 24*, 2567–2581.
42. Meng, G., Liu, S., Li, X., Krawetz, R., & Rancourt, D. E. (2010). Extracellular matrix isolated from foreskin fibroblasts supports long-term xeno-free human embryonic stem cell culture. *Stem Cells and Development, 19*, 547–556.
43. Wang, J., Liao, L., & Tan, J. (2011). Mesenchymal-stem-cell-based experimental and clinical trials: current status and open questions. *Expert Opinion on Biological Therapy, 11*, 893–909.
44. Phinney, D. G. (2012). Functional heterogeneity of mesenchymal stem cells: implications for cell therapy. *Journal of Cellular Biochemistry, 113*, 2806–2812.
45. Kawamoto, K., Konno, M., Nagano, H., et al. (2013). CD90- (Thy-1-) high selection enhances reprogramming capacity of murine adipose-derived mesenchymal stem cells. *Disease Markers, 35*, 573–579.
46. Qi, J., Chen, A., You, H., Li, K., Zhang, D., & Guo, F. (2011). Proliferation and chondrogenic differentiation of CD105-positive

enriched rat synovium-derived mesenchymal stem cells in three-dimensional porous scaffolds. *Biomedical Materials, 6*, 015006.
47. Eyre, D. (2002). Collagen of articular cartilage. *Arthritis Research, 4*, 30–35.
48. Sophia Fox, A. J., Bedi, A., & Rodeo, S. A. (2009). The basic science of articular cartilage: structure, composition, and function. *Sports Health, 1*, 461–468.
49. Eerola, I., Salminen, H., Lammi, P., et al. (1998). Type X collagen, a natural component of mouse articular cartilage: association with growth, aging, and osteoarthritis. *Arthritis and Rheumatism, 41*, 1287–1295.
50. Lu, H., Hoshiba, T., Kawazoe, N., Koda, I., Song, M., & Chen, G. (2011). Cultured cell-derived extracellular matrix scaffolds for tissue engineering. *Biomaterials, 32*, 9658–9666.
51. von der Mark, K., Kirsch, T., Nerlich, A., et al. (1992). Type X collagen synthesis in human osteoarthritic cartilage. Indication of chondrocyte hypertrophy. *Arthritis and Rheumatism, 35*, 806–811.
52. Cheung, J. O., Grant, M. E., Jones, C. J., Hoyland, J. A., Freemont, A. J., & Hillarby, M. C. (2003). Apoptosis of terminal hypertrophic chondrocytes in an in vitro model of endochondral ossification. *The Journal of Pathology, 201*, 496–503.